

AERODYNAMIC NOISE REDUCTION FOR HIGH LIFT DEVICES USING MORPHING FLAP CONCEPT

Yasuhiro Tani*, **Kazuma Miyazaki***, **Shigeru Aso***, **Hiroki Ura ****, **Takeshi Ito****

*** Department of Aeronautics and Astronautics, Kyushu University, Fukuoka, Japan,**

**** Wind Tunnel Technology Center, Japan Aerospace Exploration Agency, Tokyo, Japan**

Keywords: *morphing flap, noise reduction, high lift device, wind tunnel test*

Abstract

To reduce the aeroacoustic noise of the aircraft wings with high lift devices, the morphing flap configurations, which has smoothly contoured flap surface connected smoothly to the outer main wing, were tested in 2m x 2m low-noise low-speed wind tunnel in Kyushu university. Wind tunnel test model is a half span wing model with a flexible morphing slotted flap part, at the flow condition of up to $U=40$ m/s, $Re=1.3 \times 10^6$. Aeroacoustic noise measurements were carried out using a phased array microphone system and beamforming method analysis, in addition to the aerodynamic force measurement. Four types of morphing flap configurations were compared with conventional single slotted flap configurations. The wind tunnel test result showed that the morphing flap configuration with small flap deflection at wing root section has both better high lift and lower noise characteristics, suppressing the flap side edge noise, than conventional single slotted flap configurations.

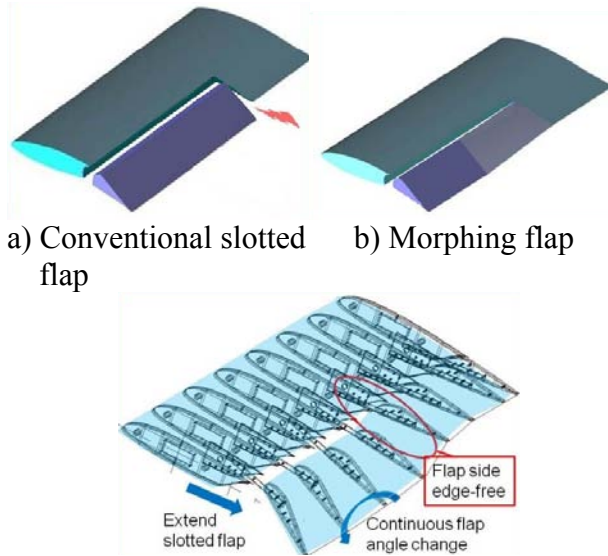
1 Introduction

Recently, environmental issue is one of the most important problems to be solved for the future air transportations. The attention has focused on the reduction of aircraft noise around the airport during take-off and landing phase. In these days, the noise from the propulsion system has been reduced, and it is of the same order of airframe noise at landing phase [1]. Therefore it is required to reduce the airframe noise for the realization of quiet transport aircrafts. Major sources of the airframe noise at landing phase

are the landing gear systems, turbulent boundary layer flow over the wings and fuselage, and flow around the high lift devices [2].

In this study, we focused on the flap side-edge noise for the slotted flaps, which is caused by the vortex flow around the flap side-edge. Various concept have been evaluated to reduce the flap side-edge noise in these years. But the noise reduction effect by the addition of small devices to the flap side-edge, such as fences, micro tabs, brush or porous surface, is not sufficient. One of the promising method is a continuous moldline (CML) flaps, which has a small fairing between the main wing trailing edge and flap trailing edge to eliminate the flap side edge, and it has been reported that CML flaps is able to reduce the noise at the flap side-edge [3]. However, this method has span wise lift change between inner flap section and outer wing section, and it causes the increase of the induced drag.

On the other hand, morphing wing is one of the promising concepts for future aircraft. As an application of the morphing wing concept, we applied it to high lift devices to reduce not only aeroacoustic noise but also aerodynamic drag. Fig. 1 shows the concept of our morphing flap, eliminating the flap side-edge itself and smooth spanwise lift distribution, comparing with the conventional slotted flap. The author's previous research showed its effectiveness and possibility [4,5,6]. In this paper, we carried out the detail noise source survey using phased array microphone and aerodynamic forces, and compared aeroacoustic and aerodynamic characteristics to obtain better morphing flap deflection angle distribution.



c) Sketch of smooth flap angle deflection

Fig. 1. Morphing Flap Concept

2 Experimental Methods

2.1 Wind Tunnel Test Facility

Wind tunnel used in this study is the low-noise low-speed wind tunnel in department of aeronautics and astronautics, Kyushu university, shown in Figs. 2 and 3. This wind tunnel is closed circuit type and has two test sections, one is an open-test section and another is a closed-type. In this experiment, we used the open-type No. 1 low-noise test section, which is in an anechoic chamber shown in Fig. 3. The size of this test section is 2 m x 2 m octagonal cross section and 5 m length. Maximum velocity is 60 m/s and the background noise level is 65 dB at 40 m/s.

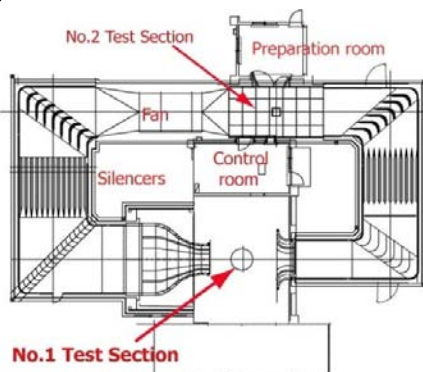


Fig. 2. Overview of Low-noise Low-speed Wind Tunnel in Kyushu University.



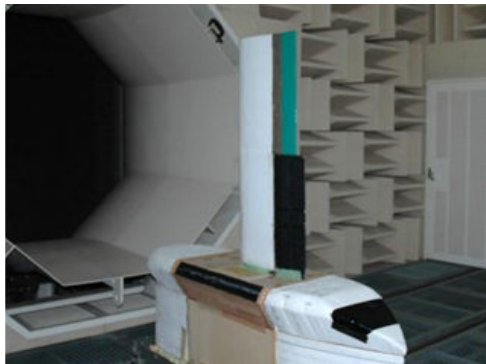
Fig. 3. No.1 Low-noise Test Section.

2.2 Test Model

The test model is a half span wing with 1150 mm span and 450 mm chord length, whose cross section is NACA23012. The wing model was supported on a half body model, which has functions as a wind shield for the force balance and a simulated simplified aircraft fuselage, placed on the wind tunnel lower wall. Fig. 4a shows the overview of the test model and the installation in the test section. The morphing flap concept was realized by a multi-rib structure, and flexible spars, shown in Fig. 4b, and elastic material surface skin. The flap part has 40% chord length of the base wing and it was installed at the trailing edge of the inner half span region of the wing. The deflection angle distribution is able to set at four spanwise locations by flap track parts. For no-deflection configuration and conventional single slotted flap configurations, all the deflection angles at four spanwise section were set uniformly shown in Fig. 5a. For the morphing flap configurations, flap deflection angle distribution is smoothly changed in spanwise and set as zero degree at 50% span location, smoothly connected from the inner to the outer wing, shown in Fig. 5b.

Flap configurations tested are listed in Table 1. Flap deflection angle δ_f was set as 0, 10, and 20 degrees uniformly for the conventional single slotted flap configurations. For the morphing flap configurations, flap angles were set at four spanwise locations; δ_{f1} , δ_{f2} , δ_{f3} and δ_{f4} , in table 1 indicate the deflection angle at

50%(flap edge), 35%, 20% and 0% span(wing root) section, respectively. All the morphing flap configuration have continuous flap deflection distribution between flap part and outer wing. Flap deflection angle of type-A changes gradually 30 degrees to 0 degree from wing root to flap edge section, and type-B has no flap deflection at both flap edges. Type-C and D have moderate flap deflection angle at root section. All the morphing flap configurations are shown in Fig. 6.

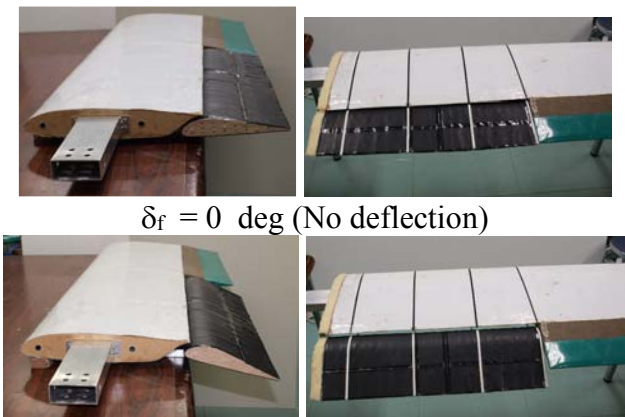


a) Overview of Model Installation



b) Flap Part Internal Structure

Fig. 4. Wind Tunnel Test Model



$\delta_f = 0$ deg (No deflection)

$\delta_f = 20$ deg

a) Conventional Slotted Flap Configuration



b) Morphing flap configuration

Fig. 5. Flap Deflection Configurations

Table 1. Test Case / Flap configurations

Flap type		Flap deflection angle , deg			
		δ_{f1}	δ_{f2}	δ_{f3}	δ_{f4}
conventional slotted flap	$\delta_f=0$ deg	0	0	0	0
	$\delta_f=10$ deg	10	10	10	10
	$\delta_f=20$ deg	20	20	20	20
morphing flap	Type A	0	10	20	30
	Type B	0	20	20	0
	Type C	0	20	20	20
	Type D	0	20	20	10



a) Type-A



b) Type-B



c) Type-C



d) Type-D

Fig. 6. Morphing Flap Deflection

2.3 Measurement Systems

In this study, we carried out aerodynamic forces measurement, noise source detection and sound pressure level measurement. Fig. 7 shows the layout of the measurement system in wind tunnel test section.

Aerodynamic forces and moments were measured using a 6-component force balance (Nissho electric works LMC-6524-2000N) mounted on the lower wall of wind tunnel test section. Noise source survey measurement was carried out using a phased array microphone system. It was developed by Wind Tunnel Technology Center (WINTeC) of Aerospace Research and Development Directorate (ARD) of Japan Aerospace Exploration Agency (JAXA)[7], and modified to fit to the Low-noise Low-speed Wind Tunnel in Kyushu university. The microphone array consists of 32 microphones (G.R.A.S. Type 40PH), data acquisition modules (National Instruments PXI-4498) and a PC. The microphones have diameter of 7 mm, frequency range of 10 to 20 kHz and dynamic range of 32 dB to 135 dB, and each has an integrated preamplifier. The A/D converter has 24 bit resolution up to 114 dB dynamic range and simultaneous sampling on all channels at the rate up to 204.8 kSamples/s.

Multi-arm-spiral arrangement was applied for the microphone array design. Three types of diameters were selected for the array, 1000 mm, 600 mm and 400 mm with similar figure, considering the target measurement frequency respectively. The arrangement of microphones for the arrays are shown in Fig. 8. Each microphone was fixed in a 10 mm thickness wooden panel and 50 mm foam sponge, and the distance between the microphone array and the wing model was set as 1900 mm. The measured sound data were analyzed using delay-and-sum beamforming method.

Besides the noise source survey, the overall sound pressure level (ASPL) was measured using a sound field microphone (RION UC-31) with a preamplifier (RION NH-04A) and a multi channel signal analyzer (RION SA-01). Frequency range of this microphone is 10 to 35 kHz, and 10 to 100 kHz for the preamplifier.



Fig. 7. Measurement System Layout.

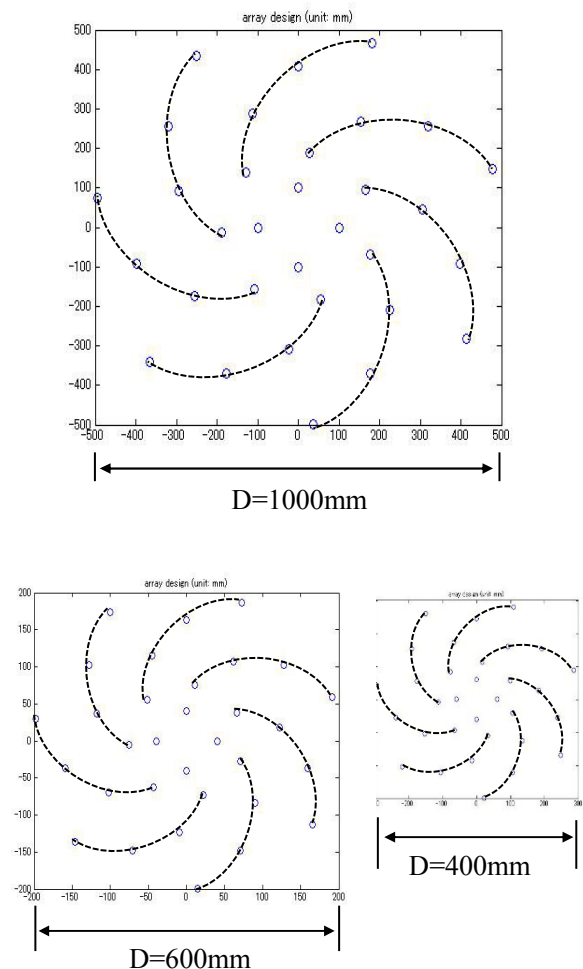


Fig. 8. Three Types of Multi-arm-spiral Microphone Array Arrangement.

2.4 Test Conditions

Test condition were selected as follows; flow velocity U was ranged from 10 to 40 m/s, and Reynolds number was 3.1×10^5 to 1.3×10^6 based on the wing chord length. The angle of attack α was set as 0 to 30 degrees.

3 Results and Discussions

3.1 Aerodynamic Force Measurement Results

Fig. 9 and 10 show the comparison of the lift coefficient C_L and drag polars, for all the flap configuration at $U=20$ m/s. Tendency of the maximum lift coefficient C_{Lmax} is reasonable for each flap configuration. Between the morphing flaps, type-A shows the highest C_{Lmax} , type-C and D shows almost same level, and type-B is the lowest. Large flap deflection angle at flap root section of type-A causes higher aerodynamic drag, and it suggests the existence of the flow separation in this region.

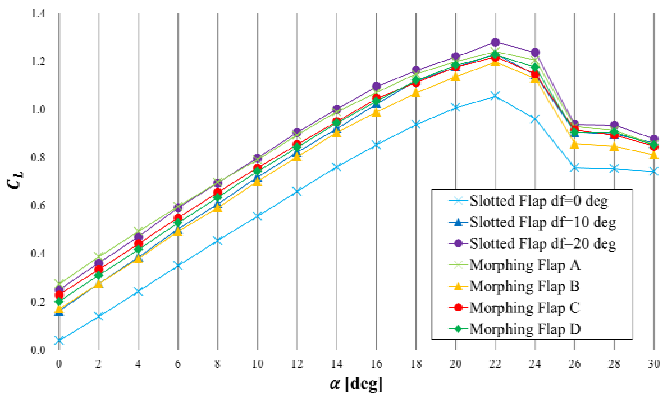


Fig. 9. Comparison of C_L , $U=20$ m/s.

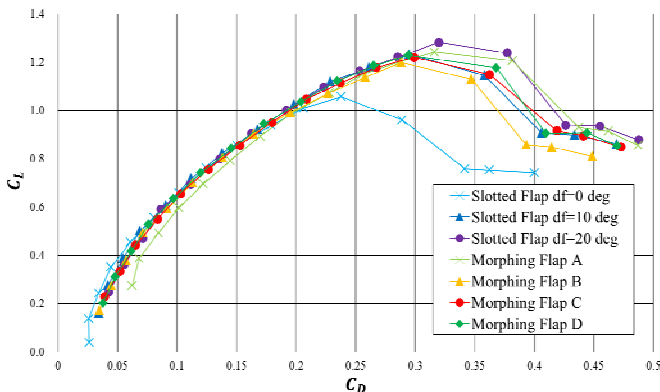


Fig. 10. Comparison of Drag Polars, $U=20$ m/s.

3.2 Microphone Array Measurements

At first, in order to understand the noise characteristics of the conventional slotted flap configuration, we examine and compare the noise source distribution for slotted flap $\delta_f=20$ degree configuration. Noise source survey results are shown in fig. 11, at the condition of $U=20$ m/s, $\alpha=14$ to 26 degrees and analysis frequency of $f_a = 4$ to 8 kHz, which is 1/3-octave band center frequency. In this measurement, 600 mm diameter microphone array was used. 22 degree of α corresponds to C_{Lmax} , and 26 degree to post stall condition.

This result clarify the existence of significant noise source at the flap side edge of conventional slotted flap, and it is realized that flap side edge noise is one of the major noise source of the wing with high lift device to be reduced. Another noise source at the flap leading edge region is also observed for 4 and 5 kHz, which is caused by the flap slot flow. The frequency of this noise source is lower than that of flap side edge.

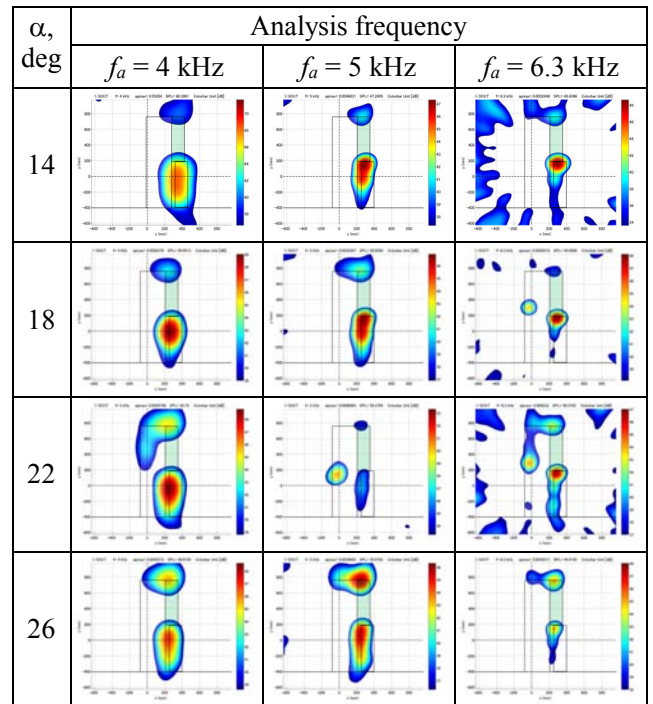


Fig. 11. Noise Source Survey Results of Conventional Slotted Flap $\delta_f=20$ deg, $U=20$ m/s.

Figure 12 shows the comparison of noise survey results of the various flap configurations for the frequency f_a range of 4 kHz to 8 kHz, at the condition of $U = 20$ m/s and $\alpha = 14$ degrees.

For the conventional single slotted flap configurations, larger flap deflection angle causes significant noise source at the flap side edge, while no flap side edge noise was observed for $\delta_f = 0$ degree case. For $\delta_f = 10$ degree configuration, noise source was observed at flap leading edge region at 4 kHz, and at the flap side edge for the frequency of 5 to 8 kHz. When the flap deflection angle was set as $\delta_f = 20$ degree, all the noise level becomes higher than that of $\delta_f = 10$ degree configuration.

The noise survey results for the morphing flap configurations indicates the suppression of the flap edge noise for all four configurations. For the frequency of 4 kHz, noise at the flap slot region still exists. However, noise source for the higher frequency was weakened on the whole. Furthermore, in this figure, small noise sources were detected at the flap slot region for 5 and 6.3 kHz frequency. It is likely to be due to the flap track parts to be used to fix the flap part to the main wing. The difference among the noise characteristics of these four types of morphing flap configuration is to be small from this result. Therefore, these data imply that this type of morphing flap concept is effective to suppress the flap side edge noise.

Figure 13 shows the comparison of the noise source for the range of angle of attack from 10 to 22 degrees, at the condition of $U = 20$ m/s and f_a is 8 kHz. Similarly as indicated in Fig. 12, significant noise source at the flap side was observed for the conventional single slotted flap configurations of $\delta_f = 10$ and 20 degrees. The flap side edge noise was observed not only for high lift condition, but also for low lift condition. In this figure, additional noise sources at the wing leading edge in the middle span location were observed at $\alpha = 22$ degrees for all the flap configurations. As fig. 8 indicates, The angle of attack for the maximum lift coefficient for these configurations are around 22 degrees. Therefore, this is because of boundary layer separation at the wing leading edge. Furthermore, the results of type-A and C

morphing flap and $\delta_f = 20$ degree conventional flap configuration indicate small noise source at the flap leading edge position in wing root section. The flap deflection angle at wing root is relatively large for these configurations; 20 degree for type-C morphing flap and $\delta_f = 20$ degree conventional flap configurations, and 30 degree for type-A morphing flap. Therefore, this noise source is caused by the flow separation at the wing root section.

3.3 SPL Measurement Results

Fig. 14 shows the comparison of overall sound pressure level, ASPL, measured by the sound field microphone, for all the configurations at $U=20$ m/s. Conventional slotted flap $\delta_f = 20$ degrees and morphing flap type-A configurations indicate higher noise level than others because of the higher lift characteristics. Fig. 15 shows ASPL comparison versus lift coefficient. Figs. 9 and 10 show that conventional slotted flap $\delta_f = 20$ degree and morphing flap type-A configurations have good high lift characteristics, though, fig. 14 shows these configurations have higher noise level for the specified lift conditions. Therefore, this data imply that morphing flap type-B and D has both high lift characteristics and low noise characteristics at high lift condition.

4 Conclusions

In this paper the effect of flap side edge noise reduction by morphing flap concept have been investigated experimentally. Detailed measurement of noise source survey using a phased array microphone system and aerodynamic characteristics showed that the flap side edge noise and overall sound pressure level can be reduced by the proposed morphing flap concept, maintaining high lift characteristics. Especially for the high lift condition, morphing type-B and D, which have the small flap deflection angle at wing root section, have both high lift and low noise characteristics.

Acknowledgements

This work was supported by MEXT/JSPS KAKENHI Grant Number(23560956).

References

- [1] Dobrzynski, Almost 40 years of airframe noise research: what did we achieve?, *Journal of aircraft*, Vol. 47 No. 2, pp. 353-367, 2010.
- [2] Streett C. L. Numerical simulation of a flap-edge flowfield, AIAA-98-2226, 1998.
- [3] Streett C. L., Casper J. H., Lockard D. P., Khorrami M. R., Stoker R. W., Elkoby R., Wenneman W. F., and Underbrink J. R. Aerodynamic noise reduction for high-lift devices on a swept wing model, *44th AIAA Aerospace Sciences Meeting*, Reno, NV, AIAA-2006-212, 2006.
- [4] Tani Y., Matsuda Y., Doi A., Yamashita Y., Aso S., and Ito T. Experimental study of the morphing flap as a low noise high lift device for aircraft wing, ICAS2012-9.11.3, 2012.
- [5] Miyazaki K., Yamashita Y., Tani Y., Aso S., Ura H., and Ito T., A study on noise characteristics of morphing flap using phased array microphone, *Proc JSASS Western Branch Conference 2013*, Yamaguchi, Japan, JSASS-2013-S009, 2013.
- [6] Tani Y., Yamashita Y., Miyazaki K., Aso S., Ura H., and Ito T. Morphing flap concept to reduce the flap side edge noise for aircraft wing slotted flaps, *Proc AIAA SciTech 2014*, AIAA-2014-0019, 2014.
- [7] Ito T., Ura H., Nakakita K., Yokokawa Y., Ng W. F., Burdisso R. A., Iwasaki A., Fujita T., Ando N., Shimada N., and Yamamoto K. Aerodynamic/aeroacoustic testing in anechoic closed test sections of low-speed wind tunnels, AIAA 2010-3750, 2010.

Contact Author Email Address

mailto:tani@aero.kyushu-u.ac.jp

Copyright Statement

The authors confirm that they, and/or their company or organization, hold copyright on all of the original material included in this paper. The authors also confirm that they have obtained permission, from the copyright holder of any third party material included in this paper, to publish it as part of their paper. The authors confirm that they give permission, or have obtained permission from the copyright holder of this paper, for the publication and distribution of this paper as part of the ICAS 2014 proceedings or as individual off-prints from the proceedings.

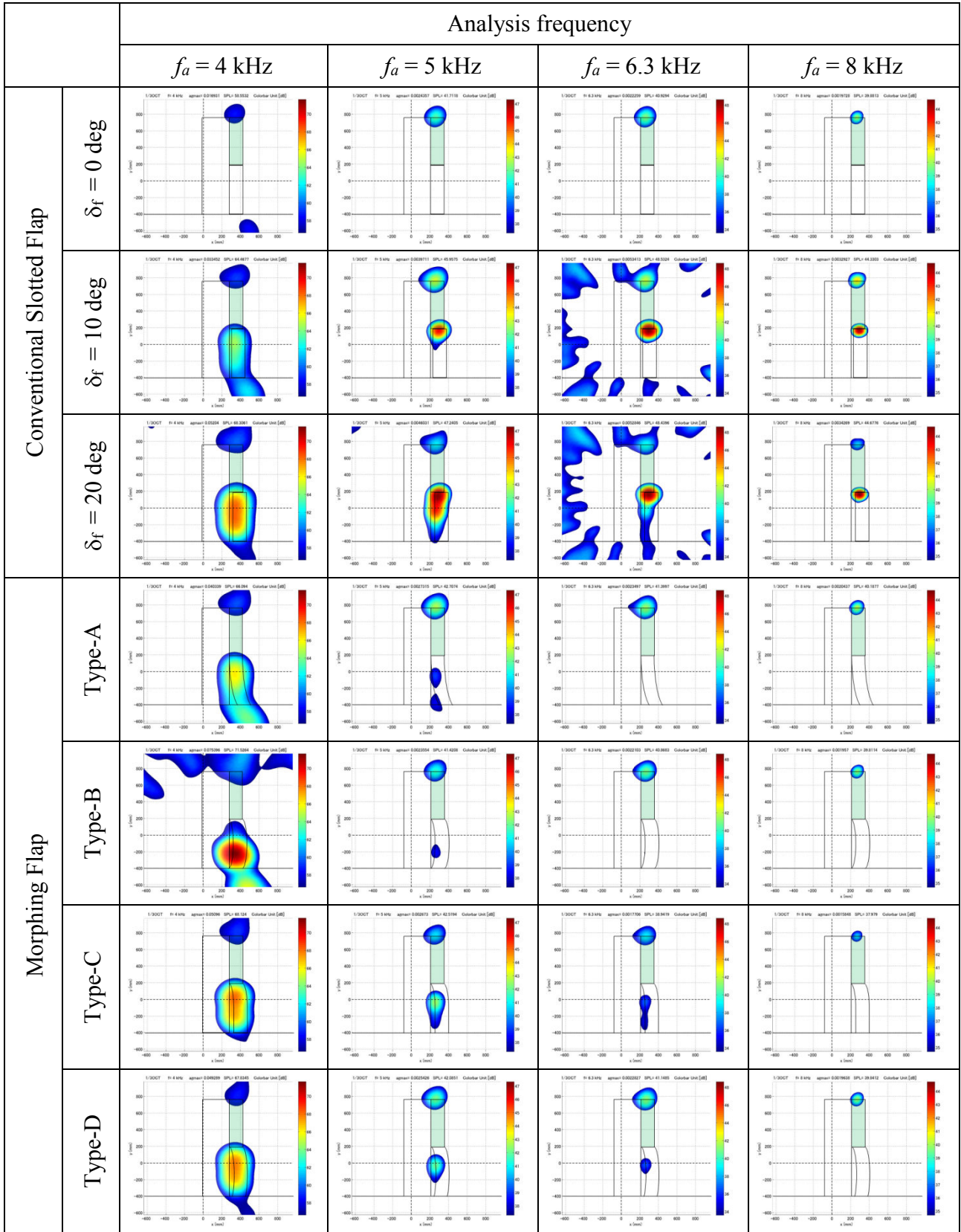


Fig. 12. Comparison of Noise Source Survey Results for $f_a=4$ to 8 kHz, $U=20$ m/s, $\alpha=14$ deg.

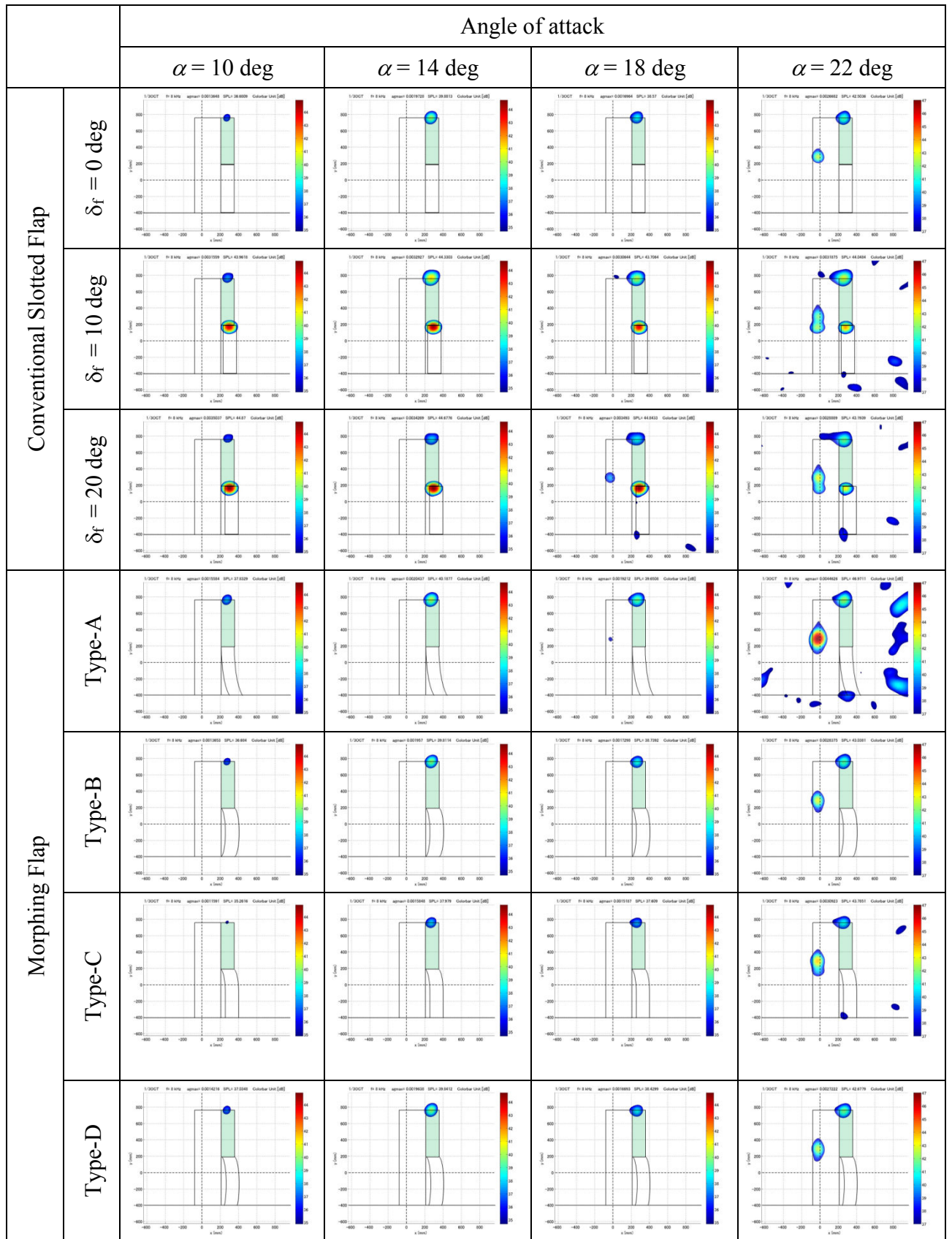


Fig. 13. Comparison of Noise Source Survey Results for $\alpha=10$ to 22 deg, $U=20$ m/s, $f_a = 8$ kHz

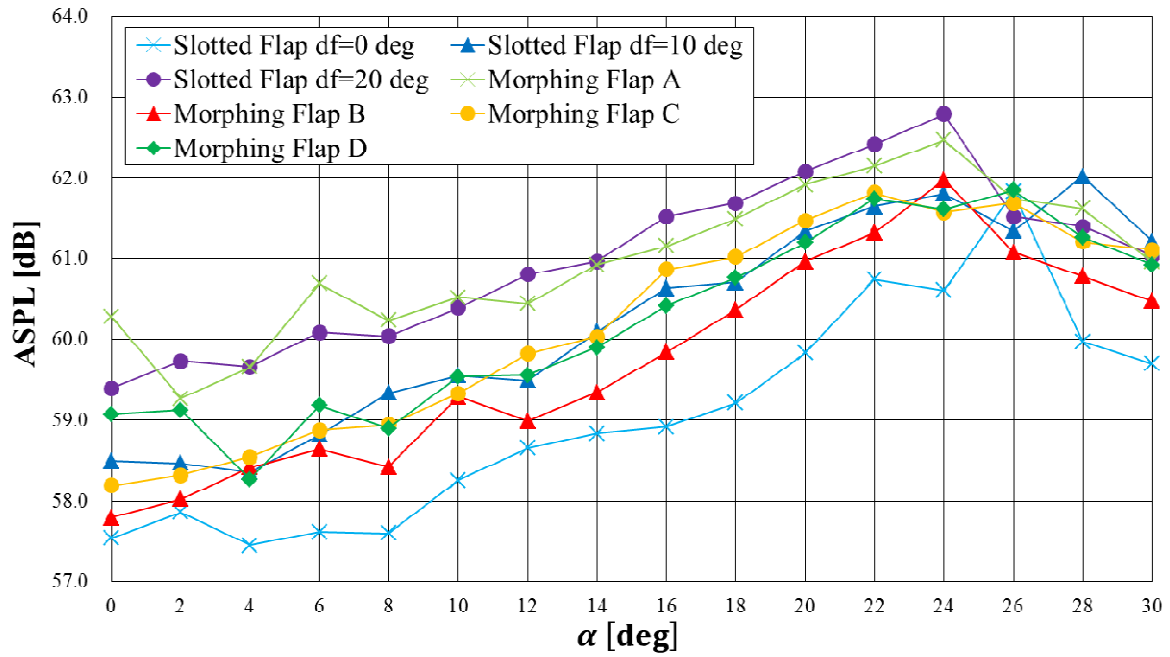


Fig. 14. Comparison of ASPL vs α , $U=20$ m/s.

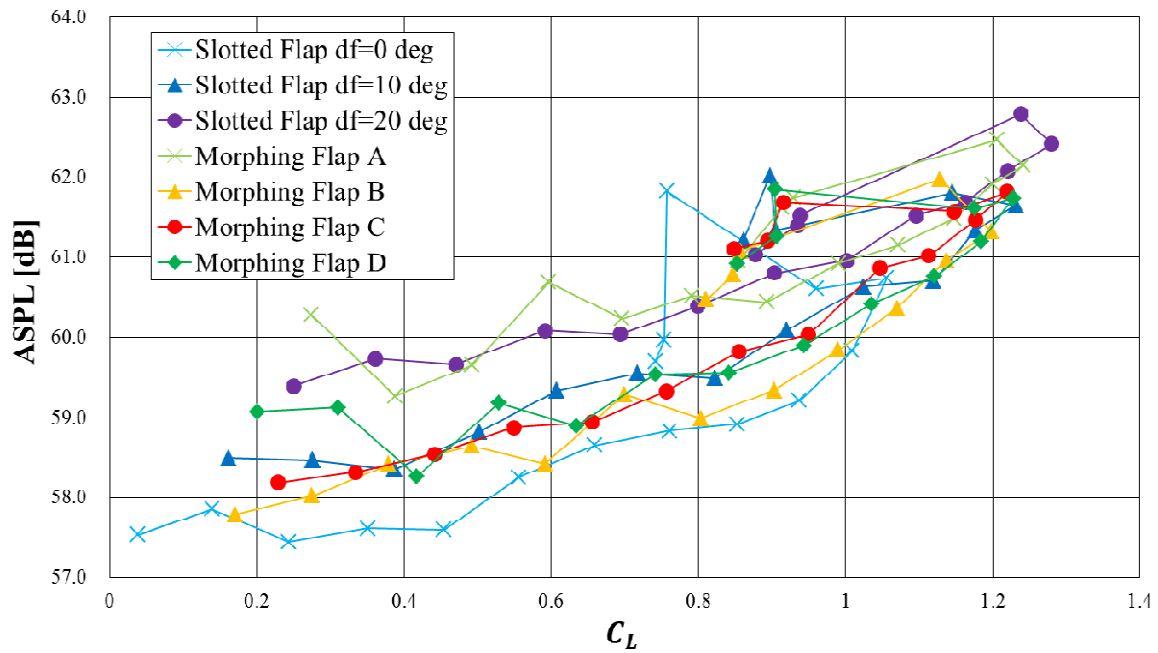


Fig. 15. Comparison of ASPL vs C_L , $U=20$ m/s.